



# Filling of Nanometric Pores with Polymer by Initiated Chemical Vapor Deposition

Manon Van-straaten, Amal Ben Hadj Mabrouk, Marc Veillerot, Christophe Licitra, Franck d'Agosto, Vincent Jousseau

## ► To cite this version:

Manon Van-straaten, Amal Ben Hadj Mabrouk, Marc Veillerot, Christophe Licitra, Franck d'Agosto, et al.. Filling of Nanometric Pores with Polymer by Initiated Chemical Vapor Deposition. *Macromolecular Rapid Communications*, 2020, 41 (14), pp.2000200. 10.1002/marc.202000200 . hal-02972734

**HAL Id: hal-02972734**

**<https://hal.science/hal-02972734>**

Submitted on 20 Oct 2020

**HAL** is a multi-disciplinary open access archive for the deposit and dissemination of scientific research documents, whether they are published or not. The documents may come from teaching and research institutions in France or abroad, or from public or private research centers.

L'archive ouverte pluridisciplinaire **HAL**, est destinée au dépôt et à la diffusion de documents scientifiques de niveau recherche, publiés ou non, émanant des établissements d'enseignement et de recherche français ou étrangers, des laboratoires publics ou privés.

**Filling of nanometric pores with polymer by initiated chemical vapor deposition**

*Manon Van-Straaten, Amal Ben HadjMabrouk, Marc Veillerot, Christophe Licitra, Franck D'Agosto, and V. Jousseume\**

M. Van-Straaten, A. Ben HadjMabrouk, M. Veillerot, C. Licitra, and V. Jousseume  
Univ. Grenoble Alpes, CEA, LETI, F-38000 Grenoble, France  
E-mail: vincent.jousseume@cea.fr

M. Van-Straaten and F. D'Agosto  
Université de Lyon, Univ Lyon 1, CPE Lyon, CNRS, UMR 5265, C2P2 (Chemistry, Catalysis, Polymers&Processes), Team LCPP Bat 308F, 43 Bd du 11 Novembre 1918, F-69616 Villeurbanne, France

Keywords: iCVD, thin films, SiOCH, low-k, poly(methacrylate)

**Abstract**

The integration of porous thin films using microelectronic compatible processes sometimes requires the protection of the interior of the pores during the critical integration steps. In this paper, the polymerization of *neo*-pentyl methacrylate (npMA) is performed via initiated chemical vapor deposition (iCVD) on a porous organosilicate (SiOCH) and on a dense SiOCH. The characterizations by FTIR, spectroscopic ellipsometry and time-of-flight secondary ion mass spectrometry (ToF-SIMS) of the different stacks show that iCVD is a powerful technique to polymerize npMA in the nanometric pores and thus totally fill them with a polymer. The study of the pore filling for very short iCVD durations shows that the polymerization in the pores is done in less than ten seconds and is uniform in depth. Then, the P(npMA) film growth continues on top of the filled SiOCH layer. These characteristics make iCVD a straightforward and very promising alternative to other infiltration techniques in order to fill the porosity of microporous thin films.

The past decade has witnessed significant advances in the ability to fabricate new porous solids from a wide range of various materials.<sup>[1-3]</sup> This has resulted in materials with unusual properties and broadened their application range beyond their traditional use such as catalysts

and adsorbents. In microelectronics, porous organosilicates thin films (SiOCH) were introduced at the beginning of the century as low-k dielectrics to isolate advanced interconnects.<sup>[4-5]</sup> More recently, these porous SiOCH were also employed as solid electrolyte in conductive bridging random access memories.<sup>[6]</sup> In addition, the porosity and vapor sorption capability of these porous thin films make these materials attractive as chemically sensitive layers in nano-electrochemical systems based on gravimetric gas sensors and miniaturized gas chromatography.<sup>[7-8]</sup> Moreover, the pore size distribution tunability of these porous organosilicates has also been used for the harvesting and detection of small molecules in liquids or for the extraction of aromatic compounds from water for on chip laboratory analyses.<sup>[9-10]</sup>

However, the integration of porous SiOCH thin films using microelectronic compatible processes is always challenging especially due to plasma-induced damage during patterning.<sup>[5,11]</sup> One possible strategy consists in protecting the structure of the porous material during the critical integration steps. A protection /deprotection strategy based on the filling of pores with an organic polymer was proposed by Frot *et al.*<sup>[12-13]</sup> This process, called the post porosity plasma protection (P4) technology<sup>[12]</sup> or the pore stuffing method,<sup>[14]</sup> is usually performed using a polymer (poly(methyl methacrylate) (PMMA) or polystyrene (PS) for instance) deposited by spin-coating on the top of the porous organosilicate thin films. Then, a treatment (usually thermal) is performed to allow the diffusion of the polymer into the open and interconnected porosity. Finally, the excess of polymer on the top of the SiOCH film is removed in a subsequent washing step.<sup>[12,15]</sup> However, with these liquid processing techniques, polymer solution viscosity, steric hindrance and lack of wettability of the surface make it difficult for the polymers to enter the pores. This often results in premature pore sealing and imperfect filling.<sup>[14,16]</sup> These limitations led Fujikawa *et al.* to study a gas phase pore stuffing processes especially for intermediate low-k materials with porosity rate lower than 20% and nanometric pore sizes.<sup>[17]</sup>

Initiated chemical vapor deposition (iCVD) is a vapor deposition method that allows the deposition of polymer thin film through a free radical polymerization.<sup>[18-19]</sup> In iCVD, a vinyl monomer and a thermally labile initiator simultaneously flow into a reactor under vacuum. The initiator is decomposed into radicals after passing through an array of heated filaments. The formed radicals then promote the free-radical polymerization at the surface of the substrate placed just below the filaments and on which monomers are adsorbed. This technique has been used to deposit a wide variety of polymer thin films including those based on methacrylate or styrenic monomer type.<sup>[18-21]</sup>

In this work, we report that iCVD is a very powerful technique to fill the microporosity of a porous SiOCH classically used by the microelectronic industry in complementary metal oxide semi-conductors (CMOS) interconnections. The pore filling by iCVD was studied on a low-k material deposited by plasma-enhanced chemical vapor deposition (PECVD). This porous SiOCH is indeed considered as the most relevant material for advanced technology nodes and is characterized by an open and interconnected porosity with a mean pore diameter close to 2 nm, as shown previously.<sup>[22]</sup>

iCVD of a film of poly(*neo*-pentyl methacrylate) (P(npMA)) was performed on porous SiOCH with an open porosity between 20 and 25%. This polymer has already been deposited by iCVD and its characteristics make it a potential candidate for a practical use in view to integrate porous SiOCH using a P4 integration scheme.<sup>[23-26]</sup> In particular, Lee *et al.* have shown that P(npMA) has a better thermal stability than P(MMA) and is completely decomposed at temperature below 400°C.<sup>[24]</sup> **Figure 1** shows the FTIR spectra of the porous SiOCH (100 nm thick) as deposited and after iCVD of 190 nm of P(npMA). The porous SiOCH is characterized by a broad band between 950 cm<sup>-1</sup> and 1250 cm<sup>-1</sup> due to Si–O–Si and a peak at 1275 cm<sup>-1</sup> related to Si–(CH<sub>3</sub>)<sub>3</sub> bending.<sup>[27]</sup> The presence of CH<sub>3</sub> is also confirmed by the existence of a small peak at 2976 cm<sup>-1</sup>. The spectrum of the iCVD deposited P(npMA) exhibits a strong signal due to carbonyl stretching (1730 cm<sup>-1</sup>) which is absent in the spectrum

of SiOCH. It shows also symmetric  $\text{CH}_2$  and  $\text{CH}_3$  vibrations ( $2870$  and  $2908\text{ cm}^{-1}$ , respectively), and antisymmetric  $\text{CH}_2$  and  $\text{CH}_3$  vibrations ( $2937\text{ cm}^{-1}$  and  $2960\text{ cm}^{-1}$ , respectively). The peaks at  $1480$  and  $1465\text{ cm}^{-1}$  can be related to C–H bending modes in P(npMA).<sup>[24,26]</sup> When P(npMA) is deposited on a porous SiOCH layer, the resulting FTIR spectrum is a combination of SiOCH and P(npMA). The C=O peak is clearly visible (at  $1730\text{ cm}^{-1}$ ) and the broadening of the  $\text{CH}_x$  band between  $2700$  and  $3000\text{ cm}^{-1}$  confirms an increase in content of hydrocarbon species. Besides, the absence of vinyl bonds ( $-\text{CH}=\text{CH}_2-$  is expected at  $1640\text{ cm}^{-1}$ ) suggests that the added species are not monomers. After subtraction of the FTIR signal of the pristine SiOCH, the resulting spectrum is similar to that of the P(npMA) indicating that the iCVD does not significantly impact the SiOCH chemical structure.

Spectroscopic ellipsometry was used to characterize the stack. The porous SiOCH and the P(npMA) optical constants are easily fitted using simple Cauchy models with a small absorption modeled by the Urbach's equation. The refractive index of the porous SiOCH is close to  $1.325$  (at  $633\text{ nm}$ ) while the polymer refractive index is close to  $1.463$ . For a stack of P(npMA) on porous SiOCH, the use of a simple bilayer optical model using the fitting parameters determined for each single layer does not lead to a good fit (Figure 1b). The best result is obtained by tuning the porous SiOCH refractive index (the SiOCH thickness is kept constant) that increases up to  $1.425$  in the example shown in Figure 1b. For comparison, the same experiments were performed using a “dense” SiOCH as underlayer (without intentional porosity added during the deposition process i.e. no porogen). In this case, the ellipsometric data of the stack P(npMA) / dense SiOCH can be fitted using a simple bilayer model without changing the fitting parameters of each individual layer (i.e. no change in the refractive index of the dense SiOCH). The increase of the refractive index of the porous sublayer after P(npMA) film growth suggests a change in the material density and therefore most probably the porosity. This effect is not observed when the P(npMA) is deposited on top of a dense SiOCH.

A careful analysis of the FTIR spectra shows that the signal of the polymer is always slightly stronger when the P(npMA) is deposited on the porous material (for a similar deposition time, see an example in **Figure 2a**). The P(npMA) chemical composition is not significantly different in both case (the FTIR spectra are very similar). This can thus be interpreted as a higher material amount deposited (higher thickness and/or higher material density) when the iCVD growth is performed on the porous SiOCH.

Figure 2b shows the area of the C=O peak as function of the P(npMA) film thickness (estimated by spectroscopic ellipsometry). The C=O concentration increases linearly with the film thickness indicating that the P(npMA) composition is constant whatever the film thickness deposited. The slopes are similar in both configurations (i.e. 0.0056), confirming that the same P(npMA) is grown whatever the underlayer (porous or not). In addition, the C=O concentration is always higher for depositions performed on porous SiOCH. The gap observed between the two types of SiOCH is constant as a function of the deposition duration. Because the FTIR spectra are not normalized, this higher C=O concentration is related to the presence of a higher amount of P(npMA). This indicates that for a similar thickness of the P(npMA) overlayer, there is always more material deposited in the case of a deposition on a porous SiOCH. All these data suggest that the pores of the porous SiOCH are first filled with P(npMA) before the growth of a P(npMA) film takes place while P(npMA) growth occurs only on the top of a dense SiOCH. The fraction of polymer contained in the porous SiOCH can be estimated by using these FTIR data. Indeed, the intercept of the linear regression for the deposition on the porous material (0.13) corresponds to an equivalent thickness of P(npMA). This equivalent thickness can be calculated by using the linear regression corresponding to the deposition on the dense SiOCH (polymer thickness =  $0.0056 \times 0.13 = 23$  nm). The polymer present in the pores therefore corresponds to a P(npMA) equivalent thickness of 23 nm. Assuming a constant polymer density, this leads to the complete filling of the 100 nm thick SiOCH having an open porosity of ~22%.

To confirm the filling of the microporous material over a significant depth, time-of-flight secondary ion mass spectrometry (ToF-SIMS) was performed on a P(npMA)/porous SiOCH/Si sample. **Figure 3a** shows the carbon (12 amu) and hydrogen (1 amu) profiles. The results obtained on as-deposited porous SiOCH are also given as reference. The filled material shows a higher carbon and hydrogen contents in comparison to the as-deposited porous SiOCH film. This composition change after iCVD can be attributed to the presence of C and H coming from the polymer into the porosity. Moreover, the profiles are relatively constant in depth until the interface with silicon (if we except the top layer from sputtering time of 0 to 500s, which corresponds to the P(npMA) layer deposited at the top of the porous SiOCH). This confirms that the P(npMA) filling is relatively uniform in depth with this deposition condition.

The previous experiments were performed using a long iCVD duration that led to P(npMA) overcoat on the porous SiOCH. We have tried to determine the minimum duration required to fill a porous SiOCH thin film (100 nm thick). **Figure 3b** shows the resulting FTIR spectra (after subtraction of the porous SiOCH on Si contribution) as function of the deposition duration. The FTIR spectra obtained for different deposition times have the same vibration bands corresponding to P(npMA). In addition, the spectra intensities are similar especially for low deposition durations (<60 s). This indicates that the pore filling occurs for very short deposition times. **It is worth noting that if the blanket coating had occluded the pore surface at the beginning of the deposition and then the iCVD layer had formed on the upper surface, the IR intensity (of the C=O peak for instance) should increase with the deposition time even for short growth durations.** **Figure 3c** shows that the refractive index of the filled SiOCH is relatively constant over the range of deposition duration investigated. Moreover, when the deposition duration is lower than 60 s, almost nothing is deposited on the top of the porous SiOCH (the thickness on top estimated by ellipsometry is lower than 2-3 nm). The iCVD process allows to fill the pores of the porous SiOCH in a very short period of time, 10 s

being the minimal iCVD duration investigated in this work. This process constitutes a very promising alternative to solution-based techniques in order to quickly fill the porosity of microporous thin films.

A conformal coverage in the nanopores at the beginning of the process could in principle explain this behavior. iCVD is known to be a technique allowing conformal depositions when appropriate process conditions are used.<sup>[28-31]</sup> It is generally accepted that high step coverage can be achieved with iCVD at low  $P_m/P_{sat}$  (typically  $< 0.1$ ),  $P_{sat}$  being the saturation pressure estimated using the Clapeyron equation at the substrate temperature and  $P_m$  the partial pressure of monomer determined by multiplying the mole fraction of monomer in the feed gas by the chamber pressure.<sup>[28-31]</sup> At higher  $P_m/P_{sat}$  conditions, deposited polymer is preferably formed at the top surface of 3D structures and this phenomenon worsens when aspect ratio increases.<sup>[30]</sup> Moreover, for small apertures (such as in the case of porous SiOCH), the deposited polymer is susceptible to easily form bottleneck-shaped pores.<sup>[31]</sup> Once even a slight bottleneck forms, the diffusion of the monomer is further hindered and the monomer can be consumed at the partially-clogged pore entrance leading to complete sealing.<sup>[31]</sup> In our work, the value used for  $P_m/P_{sat}$  is too high (close to 0.4) to expect a conformal deposition on small features (pores mean diameter of 2 nm, 100 nm thick). Moreover, a conformal coverage in the nanopores at the beginning of the process should lead to a continuous increase of the IR intensity of the bands corresponding to P(npMA) with the deposition duration even for short growth durations which is not observed in Figure 3a. This explanation, even if it cannot be completely ruled out, does not appear to be the most probable assumption.

Polymer film growth by iCVD is controlled by the adsorption of monomers at the substrate surface and their reaction with primary radicals usually produced by thermal decomposition of the initiator. The monomer adsorption behavior on a surface is often a combination of complex phenomena. For instance, it has been shown that the polymerization rate increases as a result of an increase monomer adsorption on the surface once the first polymer chains are



formed.<sup>[26]</sup> In the case of microporous material (such as porous SiOCH), the presence of nanometric pores can facilitate monomer adsorption by capillary condensation that stabilizes the monomer in a “liquid phase”. Indeed, the surface curvature in a porous media can give rise to capillary condensation. This gas-to-liquid condensation phenomenon occurs below the saturation point of the condensate and scales negatively with feature size.<sup>[32]</sup> In our experiments, depending on the process conditions, the pores can be full of monomers during the stabilization step of the monomer flow in the iCVD reactor (the monomer is flown without initiator for 180s). Ellipsometric-porosimetry (EP) is a technique that allows the measurement of the porosity of thin films by the determination of the thin film refractive index while an adsorptive molecule is filling pores.<sup>[33]</sup> **Figure 4** shows the solvent volume fractions during the adsorption and desorption of methanol sequences in the case of the porous SiOCH. The capillary condensation is observed for relative pressure (chamber pressure over saturation vapor pressure) centered at 0.55 in the EP isotherm of methanol. This EP experiment cannot be performed directly with npMA as probe using our setup but the monomer being very similar to toluene in terms of size and chemical nature, toluene can be taken as a model.<sup>[26]</sup> The capillary condensation of toluene in this type of porous SiOCH is observed for relative pressure as low as 0.1.<sup>[34]</sup> iCVD of P(npMA) was performed using a  $P_m/P_{sat}$  ratio close to 0.4. In these conditions, during the monomer flow stabilization step, the capillary condensation of the monomer in the open and interconnected porosity of the porous SiOCH can take place. After the monomer flow stabilization step, the injection of the initiator starts and leads to an almost instantaneous polymerization reaction in the pores (Figure 4b). **It is worth mentioning that a monomer stabilization step was systematically performed before the initiation to ensure a good reproducibility of the process. Although this was not checked, this step is probably crucial in the success of the pore filling.** Once the pores are filled with polymer, the polymer film growth continues on top of the filled SiOCH as on a “dense” material. The growth rate is then limited by the adsorption of monomer at the surface. Similar

behavior was recently reported by Lovikka *et al.* using an atmospheric pressure system and process conditions allowing monomers to create a thermodynamic, liquid–gas equilibrium inside nanoscaled features such as corners, fractures, below particles, and in their interstices before initiating polymerization with UV irradiation.<sup>[32]</sup> K. Ichiki *et al.* have also invoked that the deposited monomer film can be pseudo-liquid under oversaturated  $P_m/P_{sat}$  conditions on flat surface leading to good planarization effect using a sequential polymerization iCVD method.<sup>[35]</sup> Closer to our work, Nejat *et al.* have shown that iCVD is a suitable means for directly synthesizing polymers within 3D nanostructured systems such as mesoporous  $TiO_2$  nanoparticles and activated carbon with large mesopores (few tens nanometers).<sup>[36]</sup> They confirm that within a certain range of  $P_m/P_{sat}$  ratio, the diffusion of the monomers is fast enough compared to polymerization kinetics to fill efficiently the mesoporous structure with the polymer. The possibility of monomer diffusion in nano-defects of a  $SiO_2$ -like barrier layer was even demonstrated using iCVD.<sup>[37]</sup> The results obtained in our study confirm that this conclusion can be extended to microporous thin films at least in the thickness range investigated in our work.

Finally, Figure 4a shows the adsorption-desorption isotherms obtained on a porous  $SiOCH$  filled with P(npMA) by iCVD. After the iCVD process, the porosity drops to 5-6%. This low porosity is similar to those obtained on a dense  $SiOCH$  and indicates a nearly complete filling or surface sealing.<sup>[38]</sup> The adsorption and desorption isotherms of methanol are similar confirming that the methanol vapors used for EP does not interact significantly with P(npMA) in the pores. Preliminary studies show that the polymer can be removed using a thermal treatment, leading to EP isotherms similar to the pristine  $SiOCH$ .

In conclusion, this work highlights the ability of iCVD to fill the porosity of a microporous thin film with a polymer. Capillary condensation of the monomer in the nanometric pores is probably at the origin of the very quick pore filling observed with iCVD. The characterization of the pore filling for short iCVD durations shows that the polymerization in the pores of a

SiOCH thin film is complete in less than ten seconds and the quantity grown in the pores does not increase with the deposition duration. These characteristics make iCVD a very promising alternative to other infiltration techniques such as solution-based processes in order to fill the porosity of microporous thin films. It may facilitate the integration of porous SiOCH in microelectronics. The ability to fill the pores without depositing sacrificial material on the top of the porous layer is also a clear advantage in order to simplify integration approaches such as P4. Moreover, an enhancement of the mechanical and fracture properties of the filled porous materials can also be expected due to the very high level of polymer infiltration that can induce a confinement of polymer chains to dimension far smaller than their bulk radius of gyration.<sup>[39]</sup>

## Experimental Section

Porous SiOCH thin films were deposited on Si (100) substrate by plasma-enhanced chemical vapor deposition (PECVD) using a radio-frequency capacitive coupled parallel plate reactor from Applied Material (using a plasma excitation frequency at 13.56 MHz). They were obtained by co-depositing a matrix precursor and a sacrificial organic porogen, followed by a post-treatment to remove the organic porogen phase and create porosity. Diethoxymethylsilane and norbornadiene were used as silicon-based precursor for the matrix and as porogen precursor, respectively. The deposition conditions are described in previous papers.<sup>[22]</sup> Then, a UV assisted thermal treatment was performed on a hotplate at 400 °C under a broadband UV lamp in order to remove the porogen part and generate the microporosity. Details on the optimization of the curing treatment are available in reference.<sup>[40]</sup>

All iCVD-synthesized poly(*neo*-pentyl methacrylate) films were deposited in a 200 mm iCVD tool from Tokyo Electron Limited. The chamber is a vertical reactor (chemicals injected at the

top, pumping at the bottom) and is operated under reduced pressure. Typical polymer film growths were performed between 0.7 and 2 Torr. A series of resistively heated filaments are placed above a cooled substrate stage. *Neo*-pentyl methacrylate (npMA, 97%) was purchased from ABCR and tert-butyl peroxide (TBPO, 98%) was purchased from Aldrich and were used as received. High purity argon was used as carrier gas. The optimization of deposition conditions for P(npMA) films are shown in a previous paper.<sup>[26]</sup>

Thickness and refractive index of the films were measured using a MC2000 Woollam ellipsometer, at three different angles (55°, 65° and 75°) in the 193 nm - 1700 nm wavelength range. Their chemical composition and structure were characterized by Fourier Transformed Infrared spectroscopy using an Accent QS3300 system. All spectra were recorded from 400 cm<sup>-1</sup> to 4000 cm<sup>-1</sup> with a resolution of 2 cm<sup>-1</sup> and averaged over 64 scans. The background spectrum of each silicon wafer was measured prior to films deposition. Porosity was measured by ellipsometric-porosimetry (EP) using methanol as adsorptive. Experiments were performed in the visible range using an EP12 ellipsometric porosimeter from SOPRA. Ellipsometric spectra were recorded simultaneously between 1.55 and 4.13 eV with a CCD detector and an incidence angle of 60.15°.

High resolution mass depth profiles were acquired by ToF-SIMS (ToF-SIMS V from ION-TOF). A bunched 15 keV Bi<sup>3+</sup> ions was used as the primary probe for analysis (rastered area 80 x 80 μm<sup>2</sup>) and sputtering obtained using Cs<sup>+</sup> ions at low energy (500 eV, rastered area 400 x 400 μm<sup>2</sup>) in order to minimize surface damage.

### Acknowledgements

MVS gratefully acknowledge the financial support from the CEA for her PhD grant “ThèsePhare”.

Received: ((will be filled in by the editorial staff))

Revised: ((will be filled in by the editorial staff))

Published online: ((will be filled in by the editorial staff))

### References

- [1] M. E. Davis, *Nature* **2002**, 417, 813.
- [2] P. Liu, G.-F. Chen, *Porous Materials: Processing and Applications*, Edited by Butterworth-Heinemann Inc, Elsevier **2014**.
- [3] P. Van Der Voort, K. Leus, E. De Canck, *Introduction to Porous Materials*, Edited by John Wiley & Sons Ltd. **2019**.
- [4] A. Grill, *J. Vac. Sci. Technol. B* **2016**, 34, 020801.
- [5] M. R. Baklanov, P. S. Ho, E. Zschech, *Advanced Interconnects for ULSI Technology*, Edited by Wiley, **2012**.
- [6] Y. Fan, S. W. King, J. Bielefeld, and M. K. Orlowski, *ECS Trans.* **2016**, 72, 35.
- [7] E. Ollier, R. Barattin, C. Ladner, M. Petitjean, A. Bellemin-Comte, V. Gouttenoire, K. Benedetto, A. Salette, N. David, V. Jousseume, P. Puget, L. Duraffourg, E. Colinet, *Int. Conf. Solid-State Sens., Actuators and Microsyst. Proc.* **2015**, 1440-1443.
- [8] F. Ricoul, D. Lefèbvre, A. Bellemin-Comte, N. David, B. Bourlon, V. Jousseume, C. Marcoux, E. Ollier, *IEEE Sensors* **2014**, 206-208.
- [9] V. Jousseume, J. El Sabahy, C. Yeromonahos, G. Castellan, A. Bouamrani, F. Ricoul, *Microelectron. Eng.* **2017**, 167, 69-79.
- [10] L. Foan, J. El Sabahy, F. Ricoul, B. Bourlon, S. Vignoud, *Sens. Actuators B* **2018**, 255, 1039-1047.
- [11] M.R. Baklanov, J.-F. de Marneffe, D. Shamiryan, A. M. Urbanowicz, H. Shi, T.V. Rakhimova, H. Huang, P.S. Ho, *J. Appl. Phys.* **2013**, 113, 041101.
- [12] T. Frot, W. Volksen, T. Magbitang, D. Miller, S. Purushothaman, M. Lofaro, R. Bruce, G. Dubois, *Proceedings of the IEEE International Interconnect Technology Conference* **2011**, 5940272.
- [13] T. Frot, W. Volksen, S. Purushothaman, R. Bruce, and G. Dubois, *Adv. Mater.* **2011**, 23, 2828-2832.

- [14] M. H. Heyne, L. Zhang, J. Liu, I. Ahmad, D. Toma, J.-F. de Marneffe, S. De Gendt, M. R. Baklanov, *J. Vac. Sci. Technol. B* **2014**, 32 062202.
- [15] L. Zhang, J.-F. de Marneffe, M. H. Heyne, S. Naumov, Y. Sun, A. Zotovich, Z. el Otell, F. Vajda, S. De Gendt, M. R. Baklanov, *ECS J. Solid State Sci. Technol.*, **2015**, 4, N3098-N3107.
- [16] S. G. Isaacson, Y. Wang, K. Lioni, W. Volksen, T. P. Magbitang, M. Chowdhury, R. D. Priestley, G. Dubois, R. H. Dauskardt, *Adv. Funct. Mater.* **2019**, 29, 1903132.
- [17] M. Fujikawa, T. Yamaguchi, S. Nozawa, Y. Kikuchi, K. Maekawa, H. Kawasaki, R. Chanson, and J.-F. de Marneffe, *IEEE Trans. Semicon. Manuf.* **2019**, 32, 438.
- [18] K. K. Gleason, *CVD Polymers: Fabrication of Organic Surfaces and Devices*, Wiley-VCH Verlag GmbH & Co., Weinheim, Germany **2015**.
- [19] A. M. Coclite, R. M. Howden, D. C. Borrelli, C. D. Petruczuk, R. Yang, J. L. Yagüe, A. Ugur, N. Chen, S. Lee, W. J. Jo, A. Liu, X. Wang, K. K. Gleason, *Adv. Mater.* **2013**, 25, 5392–5423.
- [20] K. Chan K. K. Gleason, *Chem. Vap. Deposition* **2005**, 11, 437-443.
- [21] W. E. Tenhaeff, K. K. Gleason, *Langmuir* **2007**, 23, 6624-6630.
- [22] O. Gourhant, G. Gerbaud, A. Zenasni, L. Favennec, P. Gonon, and V. Jousseume, *J. Appl. Phys.*, **2010**, 108, 124105.
- [23] G. Ozaydin-Ince and K. K. Gleason, *Chem. Vap. Deposition* **2010**, 16, 100-105.
- [24] L. H. Lee and K. K. Gleason, *J. Electrochem. Soc.* **2008**, 155, G78-G86.
- [25] V. J. B. Jeevendrakumar, B. A. Altemus, A. J. Gildea, M. Bergkvist, *Thin Solid Films* **2013**, 542, 81-86.
- [26] L. Bonnet, B. Altemus, R. Scarazzini, M. Veillerot, F. D'Agosto, J. Faguet, V. Jousseume, *Macromol. Mater. Eng.* **2017**, 302, 1700315.
- [27] A. Grill, D. Neumayer, *J. Appl. Phys.* **2003**, 94, 6697-6707.
- [28] P. Moni, A. Al-Obeidi, K. K. Gleason, *Beilstein J. Nanotechnol.* **2017**, 8, 723-735.

- [29] A. Asatekin and K. K. Gleason, *Nano Lett.* **2011**, 11, 677-686.
- [30] S. H. Baxamusa and K. K. Gleason, *Chem. Vap. Deposition* **2008**, 14, 313-318.
- [31] S. J. Yoon, K. Pak, T. Nam, A. Yoon, H. Kim, S. G. Im, B. J. Cho, *ACS Nano* **2017**, 11, 7841-7847.
- [32] V. A. Lovikka, M. Kemell, M. Vehkamäki, M. Leskelä, *Mater. Horiz.* **2019**, 6, 1230.
- [33] M. R. Baklanov, K. P. Mogilnikov, V. G. Polovinkin, F. N. Dultsev, *J. Vac. Sci. Technol. B* **2000**, 18, 1385–1391.
- [34] C. Licitra, R. Bouyssou, T. Chevolleau, F. Bertin, *Thin Solid Films* **2010**, 518, 5140-5145.
- [35] K. Ichiki, B. Altemus, A. Gildea, J. Faguet, *Thin Solid Films* **2017**, 635, 23-26.
- [36] S. Nejati, K. K. S. Lau, *Nano Lett.* **2011**, 11, 419–423.
- [37] G. Aresta, J. Palmans, M. C. M. van de Sanden, M. Creatore, *Microporous and Mesoporous Materials* **2012**, 151, 434-439.
- [38] J. El Sabahy, J. Berthier, F. Ricoul, V. Jousseume, *Sens. Actuators B* **2017**, 258, 628-636.
- [39] S. G. Isaacson, K. Lioni, W. Volksen, T. P. Magbitang, Y. Matsuda, R. H. Dauskardt, G. Dubois, *Nature* **2016**, 15, 294.
- [40] A. Zenasni, V. Jousseume, P. Holliger, L. Favennec, O. Gourhant, P. Maury and G. Gerbaud, *J. Appl. Phys.* **2007**, 102, 094107.

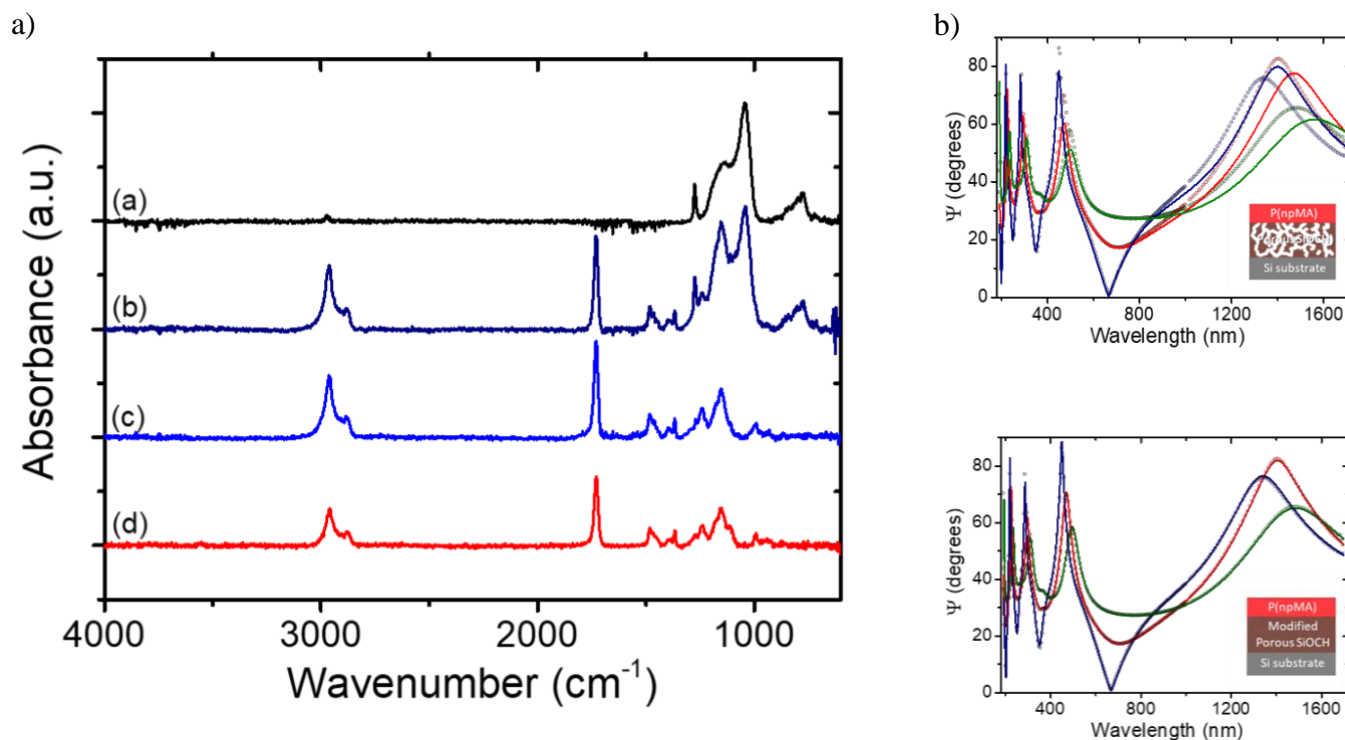


**Figure 1.** **a)** FTIR spectra of (a) as-deposited SiOCH film (100 nm thick), (b) P(npMA) (deposition for 650 s) on SiOCH, (c) P(npMA) (deposition for 650 s) on SiOCH after subtraction of the SiOCH contribution, (d) as-deposited P(npMA) (deposition duration of 650 s on Si). **b)** Evolution of the ellipsometry parameter  $\Psi$  as a function of the wavelength for different measurement angles (blue: 55°, red: 65° and green: 75°). Open circles correspond to the experimental data and lines correspond to the model. Top: a simple bilayer model using the fitting parameters determined for the different single layers does not lead to a good fit. Bottom: Fit using a bilayer model and tuning the porous SiOCH refractive index.



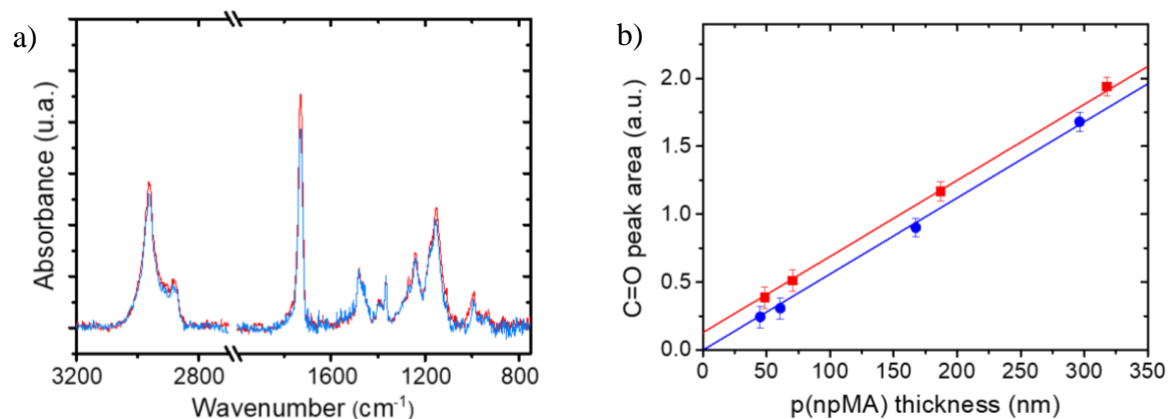


**Figure 2.** Comparison of P(npMA) film deposition by iCVD on porous SiOCH (red) and on dense SiOCH (blue) **a)** FTIR spectra (after SiOCH subtraction). **b)** Variations of the C=O peak area (at 1730 cm<sup>-1</sup>) as function of the P(npMA) film thickness (measured on top of the SiOCH thin film) for P(npMA) deposition on porous SiOCH (red square) and on dense SiOCH (blue circle).

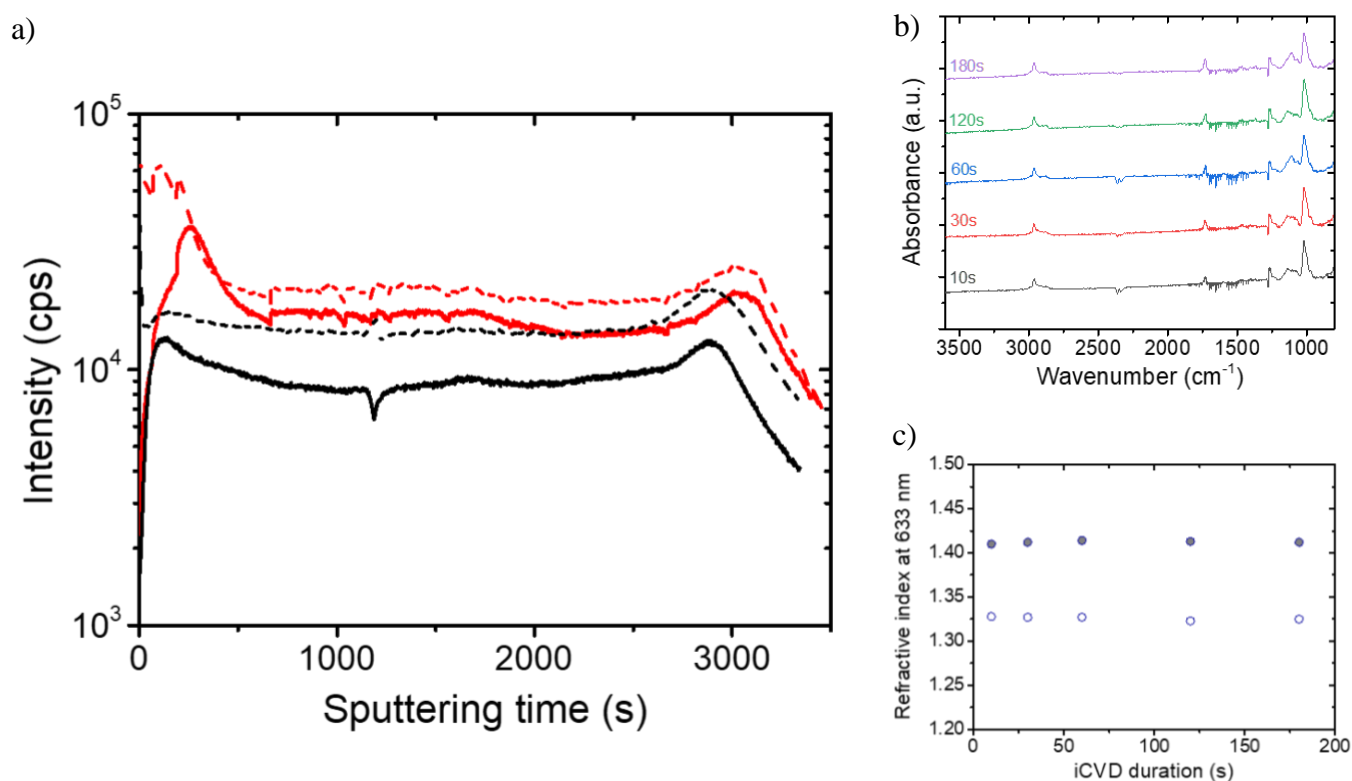


**Figure 3.** **a)** Carbon (12 amu, in black) and hydrogen (1 amu, in red) profiles obtained by time-of-flight secondary ion mass spectrometry on a P(npMA)/porousSiOCH/Si sample (dashline). The results obtained on an as-deposited porousSiOCH are also given as a reference (plain lines). **b)** FTIR spectra (after subtraction of the porousSiOCH contribution) for short iCVD deposition durations. **c)** Evolution of the refractive index of the filled SiOCH (filled circles) as a function of P(npMA) deposition duration. The refractive index of an as-deposited porousSiOCH is also shown (open circles).

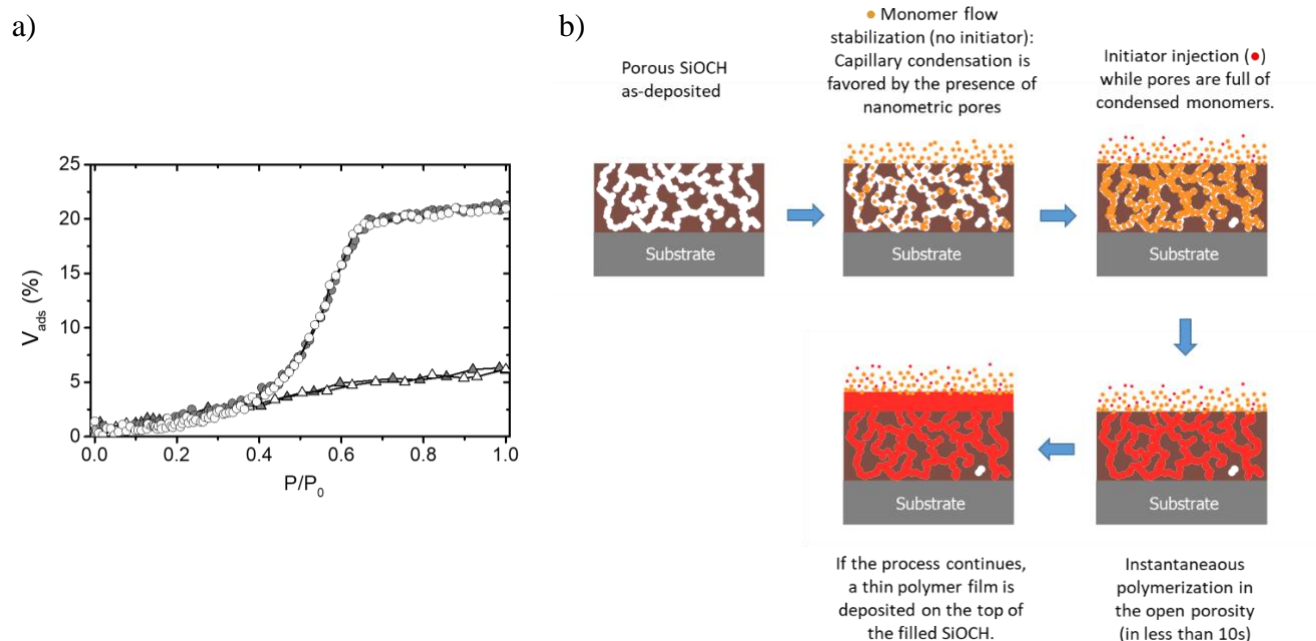


**Figure 4.a)** Methanol volume fraction deduced from ellipsometry porosimetry experiments as a function of the relative pressure of methanol (open=adsorption, gray=desorption) of a as-deposited SiOCH thin film (100 nm thick, circle) and of the SiOCH film after iCVD filling (triangle). **b)** Schematic of the micropore filling mechanism.

Initiated Chemical Vapor Deposition (iCVD) is a very powerful technique to fill with a polymer the microporosity of porous organosilicate thin films (SiOCH). Aided by the capillary condensation of monomers into the porosity, the polymerization in the nanometric pores is done in less than ten seconds and is uniform in depth.

**Keyword:** thin films

M. Van-Straaten, A. Ben HadjMabrouk, M. Veillerot, C. Licitra, F. D'Agosto, V. Jousseume

### Filling of nanometric pores with polymer by initiated chemical vapor deposition

ToC figure

